Modification of the measuring complex at the Siberian Lidar Station

V.D. Burlakov, S.I. Dolgii, and A.V. Nevzorov

Institute of Atmospheric Optics,
Siberian Branch of the Russian Academy of Sciences, Tomsk

Received June 16, 2004

We consider a modernized measurement complex of the Siberian Lidar Station for monitoring of short- and long-term variations of characteristics of stratospheric aerosol layer (SAL), ozonosphere, and the temperature of the middle atmosphere. The measurements of the SAL characteristics are performed at the wavelength of 532 nm using a receiving mirror 0.3 m in diameter. The receiving mirror with diameter of 2.2 m allows us to record molecular backscattering signals in the altitude range from 30–80 km and, simultaneously, the signals of Raman scattering from nitrogen molecules at the wavelength of 607 nm in the altitude range from 10–30 km. The simultaneous signal recording makes it possible to reconstruct the continuous temperature profile for the altitude range ~ 10–75 km. The measurements of vertical ozone distribution in the stratosphere use the method of differential absorption and scattering at the wavelength pair 308/353 nm, where lidar signals are recorded with a receiving mirror 0.5 m in diameter.

Introduction

The methods for remote laser sensing using lidar instrumentation[1,2] are now the widely used in the investigation of the atmosphere and monitoring of its state. Regular long-term measurements of a few main parameters and components of the atmosphere, which form and determine the radiative-thermal regime and the climate-ecological state of the "atmosphere–Earth's surface" system as a whole, are especially efficient. Analysis of the long-term data series of comprehensive regular measurements allows us to: develop regional empirical models of the atmospheric parameters; determine relations in the dynamics of the parameters under study; determine the effect of global atmospheric changes on regional changes; reveal short-term disturbances and gradually accumulated changes in the atmosphere under the effect of natural and anthropogenic factors; isolate periodic (season, quasi-biennial, etc.) components and predict the tendencies of the atmospheric changes.

Lidar and spectrophotometer measurements of the characteristics of stratospheric ozone and aerosol layers, gaseous components of the ozone cycles, radiative fluxes, and temperature are carried out at the world-wide International Network for Detection of Stratospheric Change (NDSC). The long-term data series of such observations are the basis for the study of mechanisms determining the changes of the ozone layer, as well as for the study of the effect of scattering and absorption properties of stratospheric aerosol of natural and technogenic origin on the processes of radiative transfer and thermal regime of the "atmosphere – Earth's surface" system.

A comprehensive approach to the study of the stratosphere has been developed at Siberian Lidar Station (SLS)[3] of the Institute of Atmospheric Optics in Tomsk (56.5°N, 85.0°E), where lidar and spectrophotometric measurements are being carried out of the characteristics of the stratospheric aerosol layer (since 1986), ozonosphere (since 1989), and temperature of the middle atmosphere (since 1995). Besides, sounding of water vapor in the troposphere and cloudiness is realized at the lidar complex of SLS. The composition and geometry of the lidar transmitting-receiving complex are changed and modified depending on the specific programs of atmospheric investigations. The technique and instrumentation for measurements are also continuously developed and improved.

The modified lidar complex is considered in this paper, which is mainly intended for stratospheric measurements. Besides, additional channels are incorporated into the complex for recording the signals of Raman backscatter (RS) from the 1st vibration-rotation transition of nitrogen molecules (the wavelength of 607 nm) at their excitation by the beam of the second harmonic of a Nd:YAG laser at the wavelength of 532 nm. Recording of the RS signals from nitrogen allows one to retrieve the profiles of temperature in the height range from about 10 to 30 km and calibrate the lidar signals of the aerosol and molecular scattering. Such a method of calibration is especially needed in the absence of data of aerological sounding on the vertical profiles of temperature in the stratosphere.

Complex automation of the computer-controlled choice and setting of the working parameters of the blocks of photoelectric recording of the lidar signals is realized in the modified lidar system. The automated optical-mechanical adjustment device is designed based on step motors. It enables transmitting laser radiation into the atmosphere and its alignment with respect to the optical axis of the receiving mirror. The technique used for retrieval of

0235-6880/04/10 756-07 $02.00

the stratospheric characteristics from the data of sounding is not considered in the paper. Only some new results are presented, which illustrate the capabilities of the complex.

1. Block-diagram of the lidar measurement complex

The general block-diagram of the existing lidar measurement complex of SLS is shown in Fig. 1. It includes two independent lidar systems: the system for measuring the characteristics of SAL and temperature of the middle atmosphere (Fig. 1*a*) and the lidar for sounding vertical profile of the ozone concentration in the stratosphere (Fig. 1*b*). With the properly replaced receiving spectral optical components, this lidar is capable of measuring humidity in the troposphere.

Principal specifications of the laser sources and receiving optical elements of the complex are presented in the Table. Then let us consider operation of separate systems of the complex.

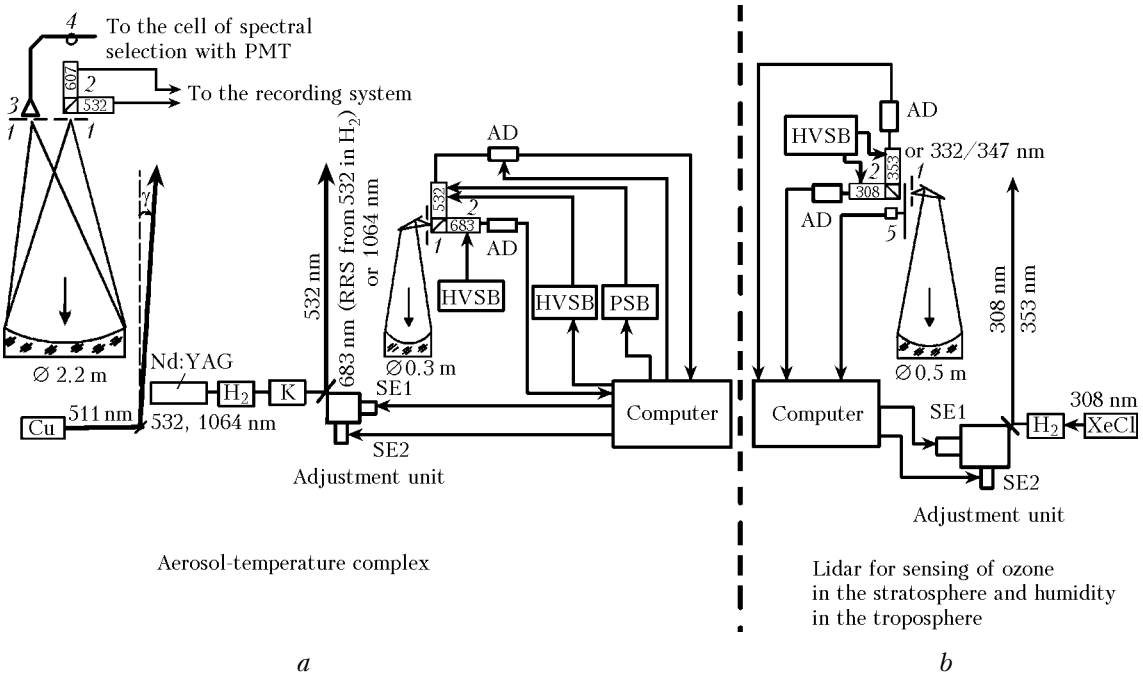

Fig. 1. The diagram of the measurement complex of the Siberian Lidar Station: field diaphragms (*1*), cells for specral selection with PMT (*2*); focon (*3*), light guide (*4*), mechanic beam chopper (*5*), Nd:YAG is solid-state laser, XeCl is excimer laser, Cu is copper-vapor laser, H_2 is the cell for SRS transformation with hydrogen, K is collimator, AD is amplifiers-discriminators, HVSB is high-voltage energy supply blocks, PSB is photoreceiver switch-on block, SE is step engines.

Table. Specifications of the lidar complex

Lidar parameters	Measured characteristics									
	aerosol					temperature	ozone	humidity		
transmitter										
Wavelength of sounding, λ, nm	511	532	628	683	1064	532	308 353	308		
Pulse energy, mJ (corresp. λ)	1	150	1	60	250	150	100 50	150		
Repetition rate, Hz (corresp. λ)	2500	20	2500	20	20	20	50–200	100		
Divergence, mrad	0.1					0.1	0.1–0.3	0.1–0.3		
receiver										
Method for sounding	Elastic backscattering						RS from N_2	Differential absorption and scattering	RS from	
									H_2O	N_2
Wavelength, nm	511	532	628	683	1064	532	607	308 353	347	332
Mirror diameter, m	2.2	0.3	2.2	0.3	2.2	2.2	2.2	0.5	0.5	
Focal length, m	10	1	10	1	10	10	10	1.5	1.5	
Interference filters										
Maximum transmission T, %	65	62	75	68	60	62	70	56 60	59	44
Transmission width at the level of 0.5T, nm	1.8	2			3.9	2	1.8	4.5 6	1.7	3

1.1. Lidar system for measuring the characteristics of the stratospheric aerosol layer and temperature of the middle atmosphere

The basis of the laser system (see Fig. 1*a*) is a model LQ514 Nd:YAG laser from "SOLAR LS" Company, Minsk, Belarus, operated at 532-nm wavelength of the second harmonic at a pulse repetition frequency of 20 Hz and pulse energy of 150 mJ. There is also a possibility of sounding at the wavelength of fundamental radiation, 1064 nm, or at these two wavelengths simultaneously. The following optical characteristics of SAL are reconstructed from the data of single-frequency sounding: vertical profile of aerosol backscattering coefficient and scattering ratio, total coefficient of the aerosol backscattering.

Regular measurements of the optical characteristics of SAL are carried out, as at the majority of lidar observatories of the worldwide network, at the wavelength of 532 nm, that makes it possible to compare the data for different geographical sites of observation. Qualitative analysis of the particle size spectrum using the Angström parameter is possible using the data of double-frequency sounding, where the pairs of wavelengths 532/1064 or 532/683 nm are used.

To determine the aerosol particle size spectrum, multifrequency sounding is episodically performed at different combinations of wavelengths: 1064, 532, 683, 511, and 628 nm, where 683 nm is the wavelength of the 1st Stokes component of stimulated vibrational Raman scattering (SRS) in a hydrogen cell pumped with the radiation at 532 nm, 511 and 628 nm are the wavelengths of generations of copper- and gold-vapor lasers, respectively. As compared with the high-energy Nd:YAG lasers, the metal-vapor lasers have less pulse energy (~ 1 mJ), that removes the effect of saturation of PMTs and distortion of the lidar signal by powerful signal from near zone of sounding. The necessary signal level against the background is reached due to high repetition rate (2.5 kHz). The output beam of the Nd:YAG laser is collimated with a lens telescope to a beam of 0.1 mrad divergence. The beams from copper- and gold-vapor lasers do not require additional collimation, because they are formed in unstable resonators, which provide for the output beam divergence of 0.1 to 0.2 mrad.

The multichannel mode of operation of the lidar with the 2.2-m-diameter receiving mirror is realized by tilting some of the sounding laser beams to a small angle $\gamma \sim 30'$ with respect to the vertical direction (Fig. 1*a* for $\lambda = 511$ nm). The position of the focal spot in the focal plane of the receiving mirror is displaced from the center at a distance of ~ 9 cm. The special cam is mounted in the focal plane of the receiving mirror for recording the lidar returns. In addition to the central diaphragm, it contains additional apertures situated on a circle of 9-cm radius concentric with the central focal spot.

To decrease the level of sky background, the field of view of the receiving system is limited by field stops having the size close to the image of the sounding beam in the focal plane. Having passed through the field-stop diaphragms, the optical laser signal comes to the cells of spectral separation that include collimating lenses, spectrum-dividing mirrors, interference filters, and lenses focusing the radiation to the PMTs. The spectral separation and recording cells are mounted either directly in the focal plane of the receiving mirror or outside it. In the latter case transmission of the optical lidar signal to the cells is being done by means of a cone concentrator (input diameter of 10 mm and output of 1 mm), optically glued with optic fibers or with bunches of optic fibers (Fig. 1*a*). The transmission of such systems reaches 70%.

A FEU-130 PMT operated in the photon counting mode is used as the detector of optical radiation in the visible wavelength range. To avoid the effect of PMT saturation by powerful signal from the near-range zone and to reduce the dynamic range of the lidar returns, the electron control of the PMT gain factor is used,[6] which makes it possible to put the PMT into the operation mode starting from a certain regulated height. Recording of signals at the wavelength of 1064 nm is realized by means of FEU-83 PMT cooled with Peltier elements to temperature about −30°C. The lidar signal from PMT transformed into current pulses comes to a wide-band amplifier and differential amplitude discriminator. The discriminator is capable of regulating the lower and upper discrimination thresholds for dark-current pulses of a particular PMT under conditions of real background light, i.e., selecting the optimal thresholds of discrimination for increasing the signal-to-background ratio. The pulses formed in the discriminator come to the pulse counters triggered synchronically with the laser pulse. The single- and two-channel counters with the accumulation of pulses in 512 or 1024 100-m long height intervals are used, i.e., recording of signals is provided up to the height of 50 or 100 km with the spatial resolution of 100 m.

In sounding the SAL at the wavelengths of 532 and 683 nm, the optical backscatter signals are collected with a receiving mirror of 0.3-m diameter. Sufficient signal-to-noise ratio is kept in this case up to the heights in excess of 30 km. The receiving telescope with the primary mirror of 2.2-m diameter is capable of recording the signals of elastic backscatter at the wavelength of 532 nm up to the heights above 70 km (Fig. 2).

The intensity of the lidar signal above 30 km, where aerosol is practically absent (at least, under background conditions in the long-term absence of powerful volcanic eruptions) is determined by the molecular scattering, that makes it possible to retrieve the molecular density and temperature of the middle atmosphere from these signals, because the air density linearly depends on temperature. Time behavior of the vertical distribution of density (temperature) allows one to study the wave

processes, the so-called internal gravity waves (IGW). Recording of the weak Raman signals from nitrogen at the wavelength of 607 nm is also performed with the same receiving mirror of 2.2-m diameter. The signal is recorded up to the height of ~ 30 km (see Fig. 2).

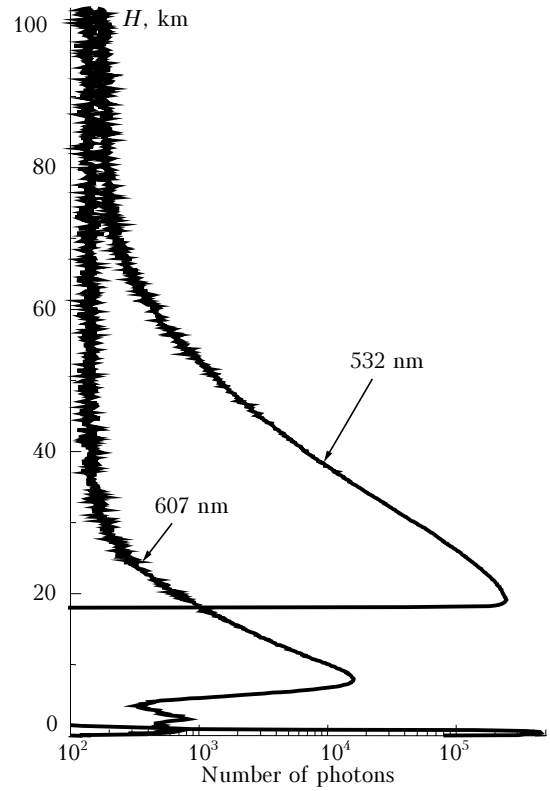

Fig. 2. Lidar signals of elastic (532 nm) and Raman (607 nm) scattering recorded on March 18, 2004 with the receiving mirror of 2.2-m diameter. The electron blocking of the PMT for the signal at 532 nm works up to 18-km height.

The main advantage of the Raman lidar is that the signal in this case does not have direct contribution of the aerosol scattering, i.e., the number of the recorded photons is directly proportional to the molecular density of the atmosphere, that makes it possible to retrieve the vertical profile of temperature. Thus, simultaneous determination of temperature from the signals of elastic molecular scattering (532 nm) and Raman signals (607 nm) makes it possible to obtain the temperature profile in the entire stratosphere and up to the heights in the mesosphere.

The developed aerosol lidar complex is also used for sounding of cloudiness in day and night time, including clouds of the upper level through the lower cloudiness.[5] The coaxial optical arrangement of the lidar receiver-transmitter is used in this case. Signal recording in the photon counting mode allows one to study the dynamics of optical and geometrical characteristics of cloudiness with temporal resolution of 3–4 s. Daylight measurements are carried out at the wavelength of 1064 nm, the high-frequency (2.5 kHz) copper-vapor laser (511 nm) is used for nighttime measurements. High pulse repetition rate of this laser under conditions of low nighttime sky background provides the informative level of the lidar signal with averaging over 1000 shots. Temporal resolution of measurements is 1 s.

The mobile version of the lidar based on a Nd:YAG laser and the receiving mirror of the diameter of 0.3 m has been designed for climatological investigations of the SAL characteristics over different geographical regions. The lidar has compact block construction and can be delivered to the measurement site by any kind of transport. The lidar showed high reliability in operation onboard a ship on Irtysh River in the region of Omsk in 2001 and as a stationary instrument during field measurements in 2001–2003 in the regions of Omsk, Surgut, Norilsk, and Lake Baikal. The results of lidar investigations of the background stratospheric aerosol characteristics over different regions of Siberia are published in Ref. 7.

1.2. Lidar for measuring the vertical distribution of stratospheric ozone and humidity in the troposphere

Lidar measurements of the vertical distribution of the ozone concentration in the stratosphere are carried out using the method of differential absorption of backscattered energy at the wavelengths of $\lambda_{on} = 308$ and $\lambda_{off} = 353$ nm, where 308 nm is the wavelength corresponding to the fundamental frequency of a XeCl excimer laser radiation (model LPX 120i Lambda Physik), 353 nm is the first Stokes component of the SRS excited with radiation at 308-nm wavelength in hydrogen. The lidar signals are collected with a receiving mirror of 0.5-m diameter (see Fig. 1) and detected with an R7207-01 PMT followed by Hamamatsu C3866 amplifier-discriminators. This PMT has higher quantum efficiency and fast-response as compared with those of a FEU-130 PMT. To remove the intense signal from the near-range zone, the mechanical beam-chopper is used. The energy potential of the lidar makes it possible to retrieve the profiles of the ozone concentration in the height range from 14 to 40 km.

Raman signals from water vapor (347 nm) and nitrogen (332 nm) molecules are present in the spectrum of the backscatter excited by a laser pulse at the wavelength of 308 nm. These signals are recorded using a coaxial optical arrangement of the lidar transmitter-receiver. In this case, the spectral optical components (spectral divider and interference filters) for 308 and 353 nm wavelengths are changed for those at 347 and 332 nm. To suppress the contamination of Raman signals by the wing of the Rayleigh scattering line at the sounding wavelength of 308 nm, an additional filter is used based on a 10-mm thick absorbing cell filled with acetone, which absorbs radiation at 308 nm and transmits that

at 332 and 347 nm. The vertical distribution of water vapor in the troposphere is determined using the ratio of the Raman lidar signals from water vapor and nitrogen as the mixture ratio.[4]

2. Automation of the control of operation of the system of photoelectron recording and optical-mechanical units of the lidar

The voltage at PMT, levels of the discrimination thresholds, the height of putting PMT into recording regime are set from the keyboard of a computer. The device for setting and regulation of the values of the enumerated parameters is linked to the computer by means of the three-channel output analog port designed as a separate card in the IBM PC standard. The block-diagram of the analog port is shown in Fig. 3.

The output analog port consists of the address selector, which selects one of three channels by corresponding address and transmits to the block of analog-to-digital converters (ADC). The block ADC forms the necessary levels of voltage, which are transmitted to the controlling blocks of the lidar.

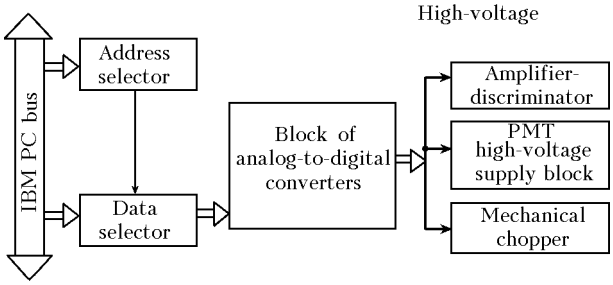

Fig. 3. Block-diagram of the three-channel output analog port.

The process of adjustment of the optical axes of the lidar transmitter-receiver, i.e., providing of recording the lidar signals from the maximum height of sounding is realized by means of an automated optical-mechanical adjustment unit (see Fig. 1) which is designed based on the step motors DSI 200-1. The block-diagram of the automated adjustment unit is shown in Fig. 4.

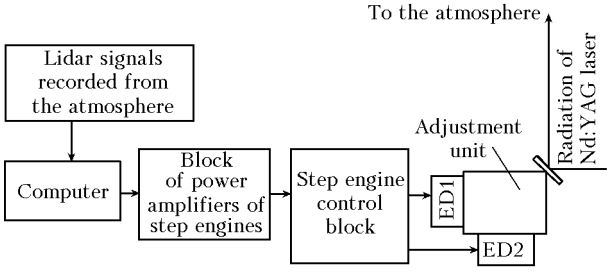

Fig. 4. Block-diagram of the automated adjustment unit.

Control of operation of the step motors is performed by means of the control block designed as a separate card in the IBM PS standard. The control block forms the pulses and the voltage levels determining the direction of rotation of the motor shafts. Then they are transmitted via a cable to the block of power amplifiers. To remove the effect of electromagnetic interference on the operation of motors, the control block works with the load of 50 Ω.

The block of power amplifiers of the step motors forms and amplifies the control pulses, which come to the coils of the step motors. The shafts of the step motors are connected with the adjustment screws of the unit by means of cogged wheels. Operation of the control block is realized by means of the software module, which is involved into the software package intended for accumulation and preliminary processing of the lidar signals. Thus, one can observe the lidar signal in real time on the computer display and adjust the lidar transmitter-receiver from the keyboard.

Before installation of the adjustment unit, the estimates were carried out of the displacement of the laser beam depending on the number of pulses sent to the step motors. They have shown that the beam deviates during one step of rotation of the motor shaft to 0.034 mrad, that corresponds to motion of the image of the sounded volume in the focal plane of the receiving mirror of the diameter of 0.3 m to the distance of 0.034 mm and to the distance of 0.34 mm for the mirror with the diameter of 2.2 m. Hence, application of the automated adjustment unit makes it possible to perform fine tuning of the lidar to the maximum height of sounding.

To make tuning of the lidar easier, the software module was created for automated adjustment of the direction of the laser radiation to the maximum height of sounding. The program operates as follows. When starting the program, initial installation of the direction of the laser beam is realized vertically up by the counter of steps, which then is stored in the computer memory after the initial manual adjustment. Then scanning of the laser beam begins first along one coordinate (both in forward and reverse direction) and then along the other, and the current height of sounding is analyzed. The cycles of steering the laser beam are being repeated unless the maximum sounding height is reached. Once the adjustment process has been finished, the program module exits to the main menu of the program, then one can start accumulation of lidar signals.

3. Some measurement results

The results of long-term investigations of the characteristics of stratospheric aerosol and ozone layers both under background conditions and under conditions of disturbance of the stratosphere by a powerful volcanic eruption are presented in Refs. 2, 7, 13–15. Let us present here only new results showing

the information capacity of long-term lidar observations and capability of the modified lidar complex to measure temperature.

The results of long-term measurements are evidence of the fact that actual levels of the aerosol content in the stratosphere of mid-latitudes after the effect of Mt. Pinatubo (eruption in June 1991) disappeared are essentially lower than the background levels in volcanic calm period (VCP) 1989–1990. The value of the total aerosol backscattering coefficient in the stratosphere in summer and fall of 2000–2004 decreased to $5 \cdot 10^{-5}$ sr^{-1} against the mean values $(1.5–2) \cdot 10^{-4}$ sr^{-1} in 1989–1990. So, the background natural and anthropogenic levels of stratospheric aerosol can be lower than it was assumed earlier. Long-term lidar measurements in Hampton[12] (USA, 37°N, 76°W) also have shown that the actual level of the aerosol burden of the stratosphere is even lower than the level observed in VCP of 1979, which was earlier considered as the background level of the aerosol content in the stratosphere.

Determination of temperature by the modified lidar complex is based on the following physical ideas. The molecular backscattering coefficient (β_π^M) is proportional to air density (ρ), and air density linearly depends on temperature T (i.e., $\beta_\pi^M(H) \sim \rho(H) \sim T(H)$). This logical chain is realized within the sounding path parts where the lidar signal is formed only due to scattering by air molecules. This condition is fulfilled at the heights above 30 km at a negligible contribution of aerosol scattering into the lidar signal as compared with the molecular scattering or in its absence.

The temperature profile $T(H)$ shown in Fig. 5*a* is retrieved from the lidar signals shown in Fig. 2 accumulated during 1 h and 25 min. To decrease the random error at far parts of the sounding path, the lidar signals were smoothed by the method of sliding average. Application of this procedure makes the spatial resolution (ΔH) rough. But the parameters of the procedure were selected so that the value ΔH does not exceed 1.5 km.

The lidar signals $N(H)$ at the wavelength of $\lambda = 532$ nm and corresponding technique for determination of $T(H)$ from the signals of Rayleigh scattering[2,8,9] with the reference to the model[11] value of temperature at the height of 77 km were used for obtaining $T(H)$ in the height range 30 to 80 km (under conditions of the absence of aerosol). To determine the temperature profile by the technique from Refs. 2 and 10 at the heights below 30 km, the signal of Raman scattering from molecular nitrogen ($\lambda = 607$ nm) was used.

Deviations (in %) of the profile $T(H)$ in the height range 30 to 80 km from the curve obtained by its approximation by the polynomial of 6th order using the least squares method are shown in Fig. 5*b* (thick line). The deviations have complex vertical structure with the fragments similar to periodic processes, the amplitude of which increases as the height increases. The sine function with the spatial period of 10 km (thin line in Fig. 5*b*) well fits the largest periodic variations of the deviations. Such properties (the increase of the amplitude and the vertical scales from 10 km and less) are characteristic of IGW. These periodic formations transfer energy from the lower layers of the atmosphere to the upper ones. The energy of decaying IGW, can transit to the flow of ambient air, that can lead to strong temperature inversions,[16] when a smooth decrease of temperature with the increasing height in the mesosphere is quite often broken by the appearance of sharp maxima. Their vertical length is several kilometers, and the amplitude can reach 40 K.

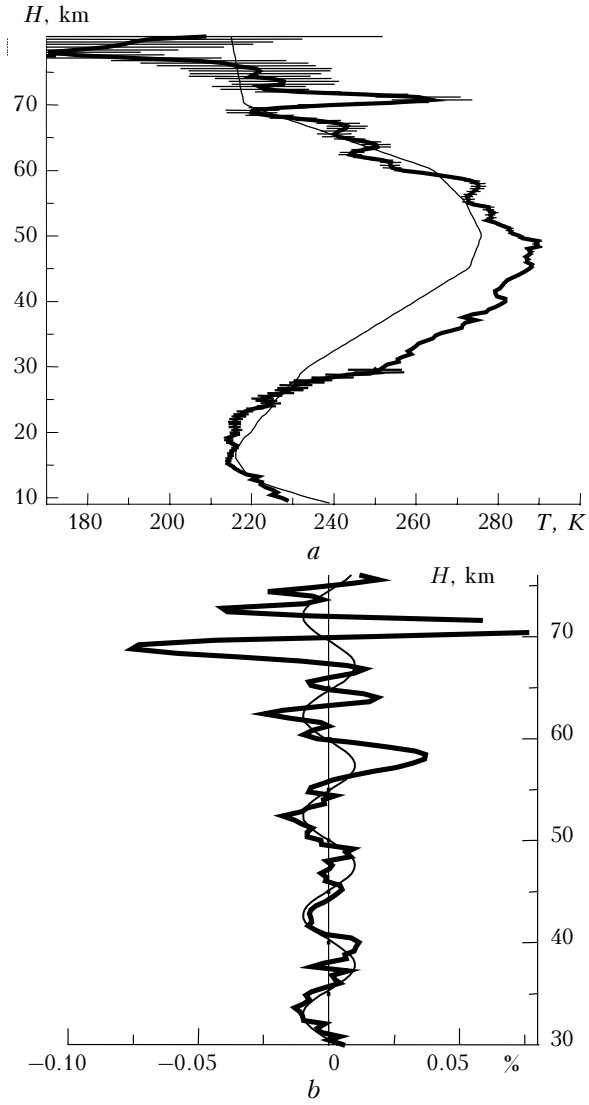

Fig. 5. Vertical profile of temperature (thick line) retrieved from the data of sounding on March 18, 2004 (see Fig. 2), model[11] profile of temperature (thin line). The random error in the corresponding height ranges is shown by horizontal lines (*a*). Deviations of the temperature profile from its approximation by polynomial of the 6th order (thick line) and sine function with the period of about 10 km in height (thin line) (*b*).

The sharp increase of temperature near 70 km in Fig. 5 can be related to the process of formation of such an inversion. It follows from the presented data that the lidar potential capabilities make it possible to investigate such important factor affecting thermodynamics parameters of the upper stratosphere as gravity waves.

Conclusion

Modification of the Siberian Lidar Station made it possible to measure the vertical profiles of temperature in the height range ~10 to 75 km from the simultaneously recorded signals of elastic molecular backscattering and the signals of Raman scattering using the same laser source and the common receiving mirror.

Complex automation is realized of the control of operation of the system of photoelectron recording and the process of adjustment of the lidar transmitter-receiver.

The designed lidar complex makes it possible to perform continuous monitoring of short-term and long-term variations of the characteristics of the stratospheric aerosol and ozone layers and temperature of the middle atmosphere. There is also a possibility of measuring the characteristics of cloudiness of lower, middle and upper levels and humidity in the troposphere.

Acknowledgments

Authors would like to thank Dr. A.V. El'nikov for useful comments and consultations during this study.

The work was supported in part by Russian Ministry of Industry and Science at the setup "Siberian Lidar Station" (registered No. 01-64).

References

1. E.D. Hinkly, ed., *Laser Monitoring of the Atmosphere* (Springer Verlag, New York, 1976).
2. V.V. Zuev, A.V. El'nikov, and V.D. Burlakov, *Laser Sounding of the Middle Atmosphere* (Rasko, Tomsk, 2002), 352 pp.
3. V.V. Zuev, Atmos. Oceanic Opt. **13**, No. 1, 84–88 (2000).
4. V.V. Zuev, V.D. Burlakov, S.I. Dolgii, A.V. Nevzorov and N.E. Orlova, Atmos. Oceanic Opt. **16**, No. 4, 344–346 (2003).
5. V.V. Zuev, M.I. Andreev, V.D. Burlakov, A.V. El'nikov, A.V. Nevzorov, and S.V. Smirnov, Atmos. Oceanic Opt. **11**, No. 5, 417–418 (1998).
6. V.L. Pravdin, V.V. Zuev, and A.V. Nevzorov, Atmos. Oceanic Opt. **9**, No. 12, 1024–1025 (1996).
7. V.V. Zuev, V.E. Zuev, V.D. Burlakov, S.I. Dolgii, A.V. El'nikov, A.V. Nevzorov, and V.L. Pravdin, Atmos. Oceanic Opt. **16**, No. 2, 111–115 (2003).
8. C.R. Philbrick, F.E. Schmidlin, K.U. Grossmann, G. Lange, D. Offermann, K.D. Baker, D. Krakowsky, U. von Zang, J. Atmos. Terr. Phys. **47**, Nos. 1–3, 159–172 (1985).
9. V.V. Zuev, V.N. Marichev, and S.L. Bondarenko, Atmos. Oceanic Opt. **9**, No. 12, 1026–1029 (1996).
10. V.V. Zuev, V.N. Marichev, S.L. Bondarenko, S.I. Dolgii, and E.V. Sharabarin, Atmos. Oceanic Opt. **9**, No. 10, 879–884 (1996).
11. I.I. Ippolitov, V.S. Komarov, and A.A. Mitsel, in: *Spectroscopic Methods for Sounding of the Atmosphere* (Nauka, Novosibirsk, 1985), pp. 4–43.
12. D.C. Woods, V.T. Osborn, P.L. Lucker, Proc. SPIE **4882**, 74–480 (2002).
13. V.V. Zuev, V.D. Burlakov, A.V. El'nikov, A.P. Ivanov, A.P. Chaikovskii, V.N. Shcherbakov, Atmos. Environ. **35**, 5059–5066 (2001).
14. V.V. Zuev, V.E. Zuev, V.D. Burlakov, S.I. Dolgii, A.V. El'nikov, and A.V. Nevzorov, Atmos. Oceanic Opt. **16**, No. 8, 663–667 (2003).
15. V.V. Zuev, S.I. Dolgii, and O.E. Bazhenov, Atmos. Oceanic Opt. **17**, No. 4, 274–278 (2004).
16. A. Hauchecorne and A. Maillard, Geophys. Res. Lett. **17**, 2197–2200 (1990).